HHS Public Access

Author manuscript

Dev Biol. Author manuscript; available in PMC 2016 August 01.

Published in final edited form as:

Dev Biol. 2015 August 1; 404(1): 66–79. doi:10.1016/j.ydbio.2015.04.025.

MED GATA factors promote robust development of the *C. elegans* endoderm

Morris F. Maduro[1,*], **Gina Broitman-Maduro**[1], **Hailey Choi**[2], **Francisco Carranza**[3], **Allison Chia-Yi Wu**[4], and **Scott A. Rifkin**[5]

[1]Biology Department, University of California, Riverside, Riverside, CA

[2]Cell, Molecular and Developmental Biology Graduate Program, University of California, Riverside, Riverside, CA

[3]MARCU-STAR Program, University of California, Riverside, Riverside, CA

[4]Graduate Program in Bioinformatics and Systems Biology, University of California, San Diego, La Jolla, CA

[5]Section of Ecology, Behavior, and Evolution, Division of Biology, University of California, San Diego, La Jolla, CA

Abstract

The MED-1,2 GATA factors contribute to specification of E, the progenitor of the *C. elegans* endoderm, through the genes *end-1* and *end-3*, and in parallel with the maternal factors SKN-1, POP-1 and PAL-1. END-1,3 activate *elt-2* and *elt-7* to initiate a program of intestinal development, which is maintained by positive autoregulation. Here, we advance the understanding of MED-1,2 in E specification. We find that expression of *end-1* and *end-3* is greatly reduced in *med-1,2(−)* embryos. We generated strains in which MED sites have been mutated in *end-1* and *end-3*. Without MED input, gut specification relies primarily on POP-1 and PAL-1. 25% of embryos fail to make intestine, while those that do display abnormal numbers of gut cells due to a delayed and stochastic acquisition of intestine fate. Surviving adults exhibit phenotypes consistent with a primary defect in the intestine. Our results establish that MED-1,2 provide robustness to endoderm specification through *end-1* and *end-3*, and reveal that gut differentiation may be more directly linked to specification than previously appreciated. The results argue against an "all-or-none" description of cell specification, and suggest that activation of tissue-specific master regulators, even when expression of these is maintained by positive autoregulation, does not guarantee proper function of differentiated cells.

[*]Corresponding author. Biology Department, University of California, Riverside, Riverside, CA, USA, 92521 (951) 827-7196, Fax: (951) 827-4286, mmaduro@ucr.edu.

Keywords

C. elegans; endoderm; cell specification; gene regulation; robustness; GATA factors; gene regulatory networks

Introduction

The robustness of embryonic development is reflected in the structure of the underlying gene regulatory networks (GRNs) that drive progenitor specification and tissue differentiation (Davidson and Levine, 2008). In the nematode, *C. elegans*, embryos follow a highly stereotyped pattern of cell divisions (Sulston et al., 1983). By the 8-cell stage, the endodermal progenitor E becomes specified to generate the 20 cells of the juvenile intestine (Sulston et al., 1983). The identification of the key regulators of E specification has made the endoderm GRN one of the best-understood networks in this animal (Maduro, 2008; Maduro and Rothman, 2002), making it an excellent system in which to probe regulatory mechanisms of developmental robustness. In this paper, through a combination of targeted lesions and detailed phenotyping, we show that disrupting the regulatory abilities of a set of putatively minor players in the endoderm GRN leads to irredeemable intestinal defects that persist through adulthood.

Specification of the E cell occurs through the sequential and combinatorial activities of a set of transcription factors (summarized in Fig. 1A). Input from the maternal factors SKN-1, the TCF protein POP-1 (with its co-activator, the divergent β-catenin SYS-1) and the Caudal-like regulator PAL-1, together cause activation of the redundant genes *end-1* and *end-3* in the early E lineage (Bowerman et al., 1992; Maduro et al., 2005b; Shetty et al., 2005). SKN-1 activates *end-1,3* in part through activation of *med-1* and *med-2* (Maduro et al., 2001). In turn, MED-1,2 bind to *end-1,3* to contribute to their activation (Broitman-Maduro et al., 2005; Maduro et al., 2002). Input from *med-1,2* is not essential for gut specification, as loss of these genes results in 15%-50% of embryos that lack endoderm (Goszczynski and McGhee, 2005; Maduro et al., 2007; Maduro et al., 2001).

POP-1 has a dual role in endoderm specification: It both activates E specification in E, and represses E specification in the sister cell of E, called MS (Shetty et al., 2005). Activation by POP-1 results from overlapping Wnt/MAPK/Src signals that occur between the 4-cell stage blastomere P_2 and EMS, the mother cell of E (Rocheleau et al., 1997; Thorpe et al., 1997). Transduction of these signals causes nuclear export of POP-1 in E, allowing the remaining nuclear POP-1 to interact with limiting amounts of nuclear SYS-1, forming a bipartite activator (Huang et al., 2007; Phillips et al., 2007). In the MS nucleus, the ratio of POP-1 to SYS-1 is high, resulting in repression of endoderm fate (Huang et al., 2007; Maduro et al., 2007; Shetty et al., 2005). A recent report identified a requirement for conserved *cis*-regulatory sites, proximal to POP-1 sites, to which POP-1/SYS-1 bind during Wnt-dependent target gene activation (Bhambhani et al., 2014). These Helper sites appear to be absent in *end-3*, suggesting that the activation component of POP-1/SYS-1 in E specification occurs primarily through *end-1* (Bhambhani et al., 2014; Robertson et al., 2014). While Wnt-activated POP-1 contributes to endoderm specification, it is not essential, as >95% of

pop-1-depleted embryos still make gut (Lin et al., 1995; Maduro et al., 2007; Maduro et al., 2005b). Like the contribution of *pop-1*, positive input into E specification by the Caudal-like factor PAL-1 can be detected by enhancement of the endoderm defect of *skn-1*-depleted embryos by *pal-1(RNAi)*, though the details of PAL-1 regulation of the *end* genes are not known (Maduro et al., 2005b).

The zygotic *end-1* and *end-3* genes together specify the endoderm fate (Maduro et al., 2005a; Zhu et al., 1997). While *end-1* and *end-3* both encode similar GATA factors, they are not completely redundant. First, mutation of either gene individually results in slightly different phenotypes (Boeck et al., 2011; Maduro et al., 2005a; Maduro et al., 2007). Second, expression of *end-3* precedes that of *end-1* and END-3 activates *end-1* (Baugh et al., 2003; Maduro et al., 2007). The *end*s activate the intestine differentiation factors *elt-2* and *elt-7*, of which *elt-2* appears to be the major regulator of intestinal identity (Fukushige et al., 1998; McGhee et al., 2009; Sommermann et al., 2010). With the exception of POP-1, which is present throughout development in many lineages (Huang et al., 2007; Lin et al., 1998), the endoderm specification factors through the *end*s are expressed only transiently, while *elt-2* and *elt-7* maintain their expression by autoregulation (and cross-regulation) for the lifetime of the animal (Bowerman et al., 1993; Fukushige et al., 1998; Hunter and Kenyon, 1996; Maduro et al., 2005a; Maduro et al., 2001; Sommermann et al., 2010). Hence, endoderm development appears to transition from specification to differentiation with the activation of *elt-2* and *elt-7*.

The paradigm for gut specification has been that it is a “binary” fate choice. In particular, loss of *skn-1* results in terminally-arrested embryos that contain either a cluster of gut-like cells or no gut cells (Bowerman et al., 1992). Studies of the Wnt/MAPK pathway also describe terminally arrested embryos as either having gut or not (Rocheleau et al., 1997; Thorpe et al., 1997). At the level of gene expression, gut specification has been proposed to occur through a threshold mechanism. While wild-type embryos accumulate sufficient *end-1* mRNA (and presumably, END-1 protein) to activate *elt-2*, embryos lacking *skn-1* activity exhibit variability in *end-1* mRNA levels, such that only those embryos reaching a threshold number of *end-1* transcripts are able to activate *elt-2* (Raj et al., 2010).

In contrast to binary specification, other studies have provided evidence that perturbation of endoderm specification can have more complex effects on the gut. First, the cell division patterns of the E lineage can be uncoupled from E fate, as has been observed with reduction of function of Wnt/MAPK components (Putzke and Rothman, 2010; Robertson et al., 2014), gain-of-function mutations in the cell cycle regulator gene *cdc-25.1* (Clucas et al., 2002; Kostic and Roy, 2002), and *end-3* single mutants (Boeck et al., 2011). Second, in embryos lacking *med-1* and *med-2*, we have observed variations in the number of *elt-2*::GFP-expressing nuclei in late-stage embryos that make gut, from only a few to greater than 30 (Maduro et al., 2007). We have interpreted aberrant gut cell numbers in *med-1,2(−)* mutant embryos to mean that MED-1,2 are required for most normal gut specification (Maduro et al., 2007), while others have used a binary definition of specification to conclude that MED-1,2 have no major role in gut specification (Captan et al., 2007; Goszczynski and McGhee, 2005).

Standard approaches have made it difficult to resolve the role of the MEDs in endoderm specification. First, RNAi of *med-1* and *med-2* by direct dsRNA injection is effective only across a narrow time interval of progeny embryos (Maduro et al., 2001). Second, there is some evidence that a component of *med* function might be maternal, such that homozygous *med-1,2(−)* embryos derived from a mother complemented for *med(+)* activity exhibit a maternal rescue of endoderm specification (Maduro et al., 2007). In those studies, a strain was made that uses a free duplication, *irDp1*, to abolish this maternal component while rescuing embryonic *med-1,2* lethality (Maduro et al., 2007). However, it has been argued that other genes inserted on *irDp1* prevent appearance of gut granules, artificially increasing the number of late-stage embryos scored as lacking gut (Captan et al., 2007). As well, other work has not detected *med-1/2* transcripts prior to the four-cell stage (Raj et al., 2010). Third, because *med-1,2(−)* embryos arrest with only partial elongation, changes in the E lineage could result from failed specification or simply because overall morphogenesis failed to occur. Loss of *skn-1* or Wnt/MAPK components also results in arrested embryos that have failed to complete morphogenesis (Bowerman et al., 1992; Lin et al., 1995; Rocheleau et al., 1997; Thorpe et al., 1997).

Here we investigate the role of the MEDs in E specification by directly assessing the consequences of loss of MED-dependent regulation of only *end-1* and *end-3*, without affecting the role of the MEDs in MS specification. We examine expression of *end-1* and *end-3* reporters in *med-1,2(−)* embryos and find that both are greatly reduced. We generated strains in which the known MED-1,2 binding sites have been mutated in the context of single-copy *end-1* and *end-3* transgenes and introduced these into an *end-1 end-3* double mutant background. We find that without MED sites, specification of gut becomes highly dependent on *pop-1* and *pal-1*, and slightly less so on *skn-1*. When MED sites have been mutated, at least some gut specification occurs in 75% of embryos, and as with prior analysis using genetic loss of *med-1,2*, ~95% of embryos make aberrant numbers of *elt-2*::GFP-expressing nuclei. These results establish that the MED sites, and hence *med-1,2*, are required for proper activation of *end-1,3* and normal gut development in the vast majority of embryos, and that the SKN-1/MED-1,2 pathway functions in parallel with both POP-1 and PAL-1. Finally, we make the unexpected finding that among those animals lacking MED sites in *end-1* and *end-3* that develop to adult stage, many exhibit defects consistent with a primary defect in the intestine. This suggests that normal adult intestine function requires robust embryonic activation of *end-1,3* by MED-1,2.

Materials and Methods

Genetics

C. elegans animals were grown on *E. coli* OP50 and handled according to standard methods. The reference strain was N2. Mutations and transgenes were as follows. *LG I: ttTi4348 [Mos], irSi10 [end-3(1-2-3-4-) + Cbr-unc-119(+)], irSi11 [end-3(1-2-3-4-) + Cbr-unc-119(+)], irSi13 [end-3(+) + Cbr-unc-119(+)], irSi25 [end-3(1+2+3+4-) + Cbr-unc-119(+)], irSi26 [end-3(1-2-3-4+) + Cbr-unc-119(+)], oxSi259 [eft-3p::GFP + Cbr-unc-119(+)]. LG II: ttTi5605 [Mos], irSi7 [end-1(1-2-) + Cbr-unc-119(+)], irSi8 [end-1(1-2-) + Cbr-unc-119(+)], irSi9 [end-1(+) + Cbr-unc-119(+)], irSi19 [end-1(1-2-) +*

Cbr-unc-119(+)], irSi20 [end-1(1-2-) + Cbr-unc-119(+)], irSi21 [end-1(1-2-) + Cbr-unc-119(+)], oxIs322 [myo-2p::mCherry::H2B + myo-3p::mCherry::H2B + Cbr-unc-119(+)]. LG III: unc-119(ed3), unc-119(ed4), unc-119(ed9), med-2(cxTi9744). LG IV: cxTi10882 [Mos], him-8(e1489), irSi24 [pept-1::mCherry::H2B + Cbr-unc-119(+)]. V: end-1(ok558), end-3(ok1448), end-3(zu247), itDf2, irIs91 [unc-119::mCherry], wIs137 [end-3::END-3[P202L]::GFP + rol-6D]. X: lon-2(e678), med-1(ok804), wIs28 [elt-2::GFP + rol-6D]. Unmapped: *teIs46 [end-1::GFP::H2B + unc-119(+)]*. Other: *irDp1(III; f) [unc-119::YFP, med-1(+), unc-32(+)], nT1 [unc-?(n754) let-?] (IV;V)*. The *ok558* and *ok1448* mutations delete the DNA-binding domains of *end-1* and *end-3*, respectively, and are null alleles for both genes; *end-1,3(−)* embryos fail to activate *elt-2* and do not make gut (Owraghi et al., 2010).

Plasmids and cloning

Cloning was performed using standard methods. MosSCI targeting vectors for *end-1* were made using pCFJ151, and for *end-3*, pCFJ352. Transgenes were constructed in steps using pUC19 and pBluescript, then introduced into the targeting vectors by restriction digestion and cloning. The MED-site mutated *end-1* reporter was constructed through two rounds of PCR and cloning using divergent, overlapping primers to introduce the indicated changes (Fig. 2D). Mutated MED sites in *end-3* were obtained using a combination of mutagenic PCR primers and *de novo* synthesis of part of the *end-3* promoter by Integrated DNA Technologies (Coralville, IA). To make a *pept-1::mCherry* reporter, 1830bp upstream of *pept-1/K04E7.2* were amplified by PCR and cloned into a vector encoding the mCherry coding region (with three introns) fused to the *his-66* coding region and the *unc-54* 3′UTR, using the vector pPD95.67 as a backbone. The recombinant transgene fusion was then cloned into the targeting vector pCFJ178. Constructs were confirmed by sequencing. Further cloning details are available on request.

Transgenesis

Chromosomal insertions were made using the MosSCI direct insertion protocol into strains EG4322, EG5003 and EG6701 with coinjection plasmids pCFJ601 (*eft-3*::Mos1 transposase) or pJL43.1 (*glh-2*::Mos1 transposase), pGH8 (*rab-3*::mCherry), pCFJ90 (*myo-2*::mCherry) and pCFJ104 (*myo-3*::mCherry), as described (Frokjaer-Jensen et al., 2012; Frokjaer-Jensen et al., 2008). For some insertions we included pMA122 (hs-*peel-1*) as an inducible negative selection marker, but in our hands it was more effective to screen for insertion candidates by absence of the coinjected mCherry markers. For some experiments, a *lon-2* mutation was introduced into the *unc-119;* Mos1 strains to facilitate injections. MosSCI *end-1* transgenes were targeted to the *ttTi5605 II* site, *end-3* transgenes to the *ttTi4348 I* site, and the *pept-1* reporter into the *cxTi10882 IV* site. Homozygous chromosomal insertion was confirmed by 100% transmission of rescue of the *unc-119* phenotype and PCR to detect the inserted transgene in its expected genomic context. We sequenced overlapping PCR products to confirm intactness of the inserted transgenes. Successful recovery of *end* transgene genomic insertions occurred at a frequency of ~20% that of the control *unc-122*::GFP targeting plasmid pCFJ68 (Frokjaer-Jensen et al., 2008). The choice to insert the *end* transgenes parallel to the *Cb-unc-119* rescue marker was deliberate, as attempts to insert transgenes in which the direction of *end* transcription was

inverted (i.e. convergent to the *Cb-unc-119* gene) resulted in high embryonic lethality following injection with very few (or no) rescued F_1s. In our hands, approximately 20% of all single-copy insertion candidates failed to breed true for *unc-119* rescue after several generations even though PCR showed these transgenes to be chromosomally inserted; such strains were eliminated from further consideration. Finally, we note that multiple independent insertions using the same targeting plasmids were indistinguishable in phenotype assays, suggesting they are identical. For simplicity, we collectively refer to the *end-1(1-2-)* insertions (*irSi7, irSi8, irSi20, irSi21*) as *Si[end-1(MED-)]* and the *end-3(1-2-3-4-)* insertions (*irSi10, irSi11*) as *Si[end-3(MED-)]*.

Reporters for *end-1* and *end-3*

The *end-1* reporter *teIs46* carries 2165 bp upstream of the predicted start codon of *end-1*, from the start of the coding region of the nearest upstream gene on the other strand, extending through the middle of the coding region of *end-1* (Shetty et al., 2005), while the *end-3* reporter *wIs137* contains the nearest upstream gene, *aip-1*, and the entire *end-3* gene with the P202L substitution (present in the apparent null allele *zu247*) in the *end-3* DNA-binding domain (Maduro et al., 2005a).

Strain construction

Worm strains were constructed by standard methods. Mutations and transgenes were combined using standard crosses with a reciprocal balancer strategy to simplify strain recovery. To introduce the *end* transgenes into the *end-1(ok558) end-3 (ok1448)* double mutant background, *myo-2::mCherry* (*oxIs322*) and *eft-3::GFP* (*oxSi259*) transgenes, inserted at the *ttTi5605 II* and *ttTi4348 I* sites, respectively, were used as balancers. We introduced *oxIs322* and *oxSi259* into an *end-1,3(−)* background rescued by an extrachromosomal array (*irEx498*) carrying *end-3(+)* and an *unc-119*::mCherry reporter (Owraghi et al., 2010). In parallel, an integrated *unc-119*::mCherry array (*irIs91 V*) was introduced into the single-copy *end* transgene strains as a balancer for the *end-1 end-3* double mutant chromosome. By crossing strains together, the absence of reporter balancers could be used for counter-selection to confirm recovery of strains homozygous for either or both *end* transgenes and the *end-1,3(−)* chromosome. For introduction of only one of the single-copy *end-1* or *end-3* transgenes into an *end-1,3(−)* background, either the *oxIs322* or *oxSi259* balancer was used as appropriate. The *end-1,3(−)* strains carrying only *end-1(MED-)* or *end-3(MED-)* single-copy transgenes were maintained by an extrachromosomal rescuing array carrying a fluorescent reporter. The *end-1,3(−); Si[end-1(MED-)]* strain could be maintained in the absence of the array, though with a very low percentage of viable progeny. A *him-8(e1489)* background was used as a source of males, and was confirmed to be absent from strains by ensuring the absence of the Him phenotype in subsequent generations. As noted in the text, the *end-1(ok558) end-3(ok1448) V; irSi[end-1(MED-)] II; irSi[end-3(MED-)] I* genotype will be abbreviated as *end-1,3(MED-)* for simplicity. To generate *itDf2* strains carrying the *end-1* and *end-3* transgenes, *oxIs322* and *oxSi259* were first introduced into an *itDf2; nT1* strain. This was then crossed with males carrying the single-copy *end-1* and *end-3* transgenes and *irIs91*, and balanced *itDf2/irIs91; end-1* transgene; *end-3* transgene hermaphrodites were obtained.

These were then self-fertilized and non-*irIs91* progeny embryos (homozygous for *itDf2*) were scored for gut.

Additional *end-1* and *end-3* expression assays in *med-1,2* mutant embryos

We constructed *med-1; med-2; irEx138 [med-1(+), unc-119::CFP]* strains carrying either *teIs46 [end-1::GFP]* or *wIs137 [end-3::GFP]*. The *irEx138* array is lost meiotically in ~2% of hermaphrodites. We singled out young hermaphrodites in groups of 20–50 for each strain and identified germline mosaics by observing plates that failed to pass the array to the first ~50 progeny as evidenced by the failure of any of the embryos to hatch, and confirmed by the absence of *unc-119*::CFP expression in any of these. Progeny embryos were then confirmed to be at a stage appropriate for expression of *end-1*::GFP or *end-3*::GFP and examined by fluorescence microscopy. We found that 27/27 *med-1,2(−); teIs46* embryos failed to express *end-1*::GFP and 31/32 *med-1,2(−); wIs137* embryos failed to express *end-3*::GFP.

RNAi experiments

RNAi by bacterial feeding was performed as described, using cDNA clones for *skn-1*, *pop-1* or *pal-1* in the *E. coli* strain HT115 (Kamath et al., 2001; Maduro et al., 2005b). Direct dsRNA injection for these same genes was performed as described (Maduro et al., 2005b). Developmental arrest was observed in >95% of progeny embryos, which were also confirmed to display the expected phenotypes by DIC for individual knockdown of *skn-1*, *pop-1* or *pal-1* (Bowerman et al., 1992; Hunter and Kenyon, 1996; Lin et al., 1998; Lin et al., 1995).

Developmental progression experiments

Twenty adults each of the *end-1,3(−); Si[end-1(+)]; Si[end-3(+)]* and *end-1,3(−); Si[end-1(MED-)]; Si[end-3(MED-)]* strains were placed on two 3-cm plates (10 per plate), allowed to lay eggs for two hours, then removed. Any embryos older or younger than the bean stage were removed. Plates were grown in parallel between 20°C-23°C. Development was monitored every two hours starting 40 hours after the eggs had been laid. Animals that had reached young adult stage as judged by vulva morphology, presence of a germline, but lacking embryos, were scored and removed.

Microscopy, imaging and scoring for gut

All phenotypes were scored at 20°C. Embryo imaging was performed as described (Owraghi et al., 2010). Staining and imaging for smFISH experiments were performed as described (Raj et al., 2010). Transcript counts were estimated from the images using custom software (Rifkin, 2011; Wu and Rifkin, 2015). The endogenous *end-1* and *end-3* mRNAs are not detected because the majority of the smFISH probes are deleted by the *end-1(ok558)* and *end-3(ok1448)* mutations (data not shown). Gut was scored as present in an embryo if a patch of gut granule-like material was observed under polarized light. We previously observed that 11–13% of embryos double mutant for *end-1* and *end-3* exhibit gut granule-like material localized to the excretory canal (Owraghi et al., 2010). However, we are able to distinguish true gut granules by confirming nuclear morphology of cells associated with

them, or expression of integrated *pept-1*::mCherry::H2B (*irSi24*) or *elt-2*::GFP (*wIs84*) reporters (Fukushige et al., 1998; Nehrke, 2003). We found that in embryos with very little gut, expression of *wIs84* becomes apparent in a small number of nuclei that appear to be in the gonad primordium based on morphology (Chang et al., 2005) and on the lack of association with gut granules. Such expression was not exhibited by *irSi24*, confirming that it is external to the gut. To score number of gut nuclei, *end-1,3(−); Si[end-1(+)]; Si[end-3(+)]; irSi24 [pept-1::mCherry::H2B]* and *end-1,3(−); Si[end-1(MED-)]; Si[end-3(MED-)];)]; irSi24 [pept-1::mCherry::H2B]* strains were grown in parallel. Late L4 stage animals were examined by fluorescence microscopy and scored for number of mCherry(+) nuclei.

Results

Expression of full-length *end-1* and *end-3* reporters is dependent on MED-1,2

Prior work has shown that *end-1* and *end-3* are activated by multiple factors (Fig. 1A) (Broitman-Maduro et al., 2005; Maduro et al., 2005a; Maduro et al., 2002; Robertson et al., 2014; Shetty et al., 2005). The promoters of both genes contain various binding sites for these factors as shown in Fig. 2A; an analysis of the frequency of these sites is shown in Table S1. We have previously shown that the DNA-binding domain of MED-1 interacts directly with binding sites in *end-1* and *end-3* of sequence 5′-GTATACTYYY-3′, and that these sites are required for GFP expression using “minimal” reporters <200bp (Broitman-Maduro et al., 2005; Maduro et al., 2002). To evaluate the requirement for *med-1,2* function in the context of full-length promoters, we examined expression of integrated, full-length *end-1* and *end-3* reporters (see Materials and Methods). We introduced these separately into a *med-1(ok804); med-2(cxTi9744)* double null mutant strain that carries *irDp1*, a free duplication rescuing the lethality of loss of *med-1* and *med-2*, and whose presence can be detected by expression of an *unc-119*::YFP transgene (Maduro et al., 2007). The partial endoderm defect of *med-1,2(−)* mutants, and the multitude of other regulatory inputs into both *end-1* and *end-3* (Fig. 2A), predicted that the expression of the *end-1* and *end-3* reporters would exhibit only a minor reduction of expression when chromosomal *med-1,2* function is lost. Contrary to this prediction, expression of both reporters was reduced to background or near-background levels in *med-1,2(−)* embryos (n=30 for each; representative embryos shown in Figs. 1B–1E). We performed similar experiments in *med-1,2(−)* strains rescued by an extrachromosomal array, rather than *irDp1*, with similar results (see Materials and Methods).

The endogenous expression of the *end*s cannot be completely absent in all *med-1,2(−)* embryos, as such embryos make gut most of the time. The failure to observe significant *end* reporter expression may be due to the multicopy nature of the transgenes, or the inability to detect very low levels of expression. We hypothesized that a more direct assessment of the contribution of MED-1,2 regulation of *end-1* and *end-3* could be made by evaluating gut specification when the MED-1,2 *cis*-regulatory sites have been mutated in the *end* genes. To perform these experiments, we cloned the complete *end-1* and *end-3* genes into separate targeting vectors for single-copy insertion by the MosSCI protocol (Fig. 2B) (Frokjaer-Jensen et al., 2012; Frokjaer-Jensen et al., 2008). The *end-1* gene contains two MED binding

sites (5′-GTATACTYYY-3′, Fig. 2C), while *end-3* contains four (Broitman-Maduro et al., 2005; Lowry et al., 2009). We made additional transgenes containing point mutations that are predicted to interfere with binding by the MED-1 DNA-binding domain (Fig. 2D) (Lowry et al., 2009). As *med-1* and *med-2* appear to have redundant function, and the DNA-binding domain of MED-2 differs from that of MED-1 by only a single amino acid, it is likely that both proteins recognize the same site.

Single-copy transgenic *end-1* and *end-3* are proxies for the endogenous loci

We inserted the *end-1* and *end-3* transgenes into defined sites on chromosomes II (*ttTi5605*) and I (*ttTi4348*), respectively, as both locations are known to be compatible with normal expression of introduced genes (Frokjaer-Jensen et al., 2012). Separate insertions mimic the endogenous *end* loci, as *end-1* and *end-3* are approximately 30 kbp apart on *LG V*, with four protein-coding genes between them, including the neural gene *ric-7* (Hao et al., 2012; Maduro et al., 2005a). We will refer to the control transgene insertions as *Si[end-1(+)]* and *Si[end-3(+)]*. Where the MED sites have been mutated in a transgene, this will be indicated as in *end-1(MED-)* or *end-3(MED-).* To refer to individual MED binding sites, a notation such as *end-3(1-2-3-4+)* would indicate that the first three sites have been mutated while the fourth is intact. The *end-1(ok558) end-3(ok1448) V* double null mutant background, common to all of the strains, will be denoted as *end-1,3(−).*

We first established that the single-copy transgenes exhibit normal levels of *end-1* and *end-3* expression. The expression patterns for both genes and for *elt-2* were consistent between N2 and *end-1,3(−); Si[end-1(+)]; Si[end-3(+)]* (Fig. 2E) and did not display any of the changes in timing or levels that occur when these genes are perturbed (Raj et al. 2010; ACW and SAR, in preparation). Hence, these transgene locations do not exhibit any gross differences in timeliness or degree of transcription.

We next tested the ability of the wild-type transgenes to complement the *end-1,3(−)* background in various configurations, as summarized in Table 1. As expected, the control *end-1,3(−); Si[end-1(+)]; Si[end-3(+)]* strain made gut 100% of the time (n>500; Fig. 3A). We found that if only the *Si[end-1(+)]* transgene is present in the *end-1,3(−)* background, 96% of embryos made gut (n=133; Fig. 3C). This genotype is equivalent to a single *end-3* mutant, which we have previously reported as 95% making gut (Maduro et al., 2005a). This result is informative: An extrachromosomal multicopy array containing *end-1(+)* restores gut to 100% of *end-1,3(−)* and *end-3(−)* embryos (Maduro et al., 2005a), showing that greatly increased dosage of *end-1* overcomes any requirement for *end-3*. In the converse experiment, the *end-1,3(−); Si[end-3(+)]* strain makes gut 100% of the time just as *end-1* single mutants do (Fig. 3D) (Maduro et al., 2005a). These results suggest that the single-copy *end-1* and *end-3* transgenes show near-normal levels of *end-1* and *end-3* expression, assayed by both rescue of endoderm and accumulation of transcripts, and are therefore good proxies for the endogenous *end* genes.

MED sites in the *end* genes are important for gut specification in a chromosomal context

We next introduced the *Si[end-1(MED-)]* and *Si[end-3(MED-)]* transgenes together into the *end-1,3(−)* background to generate a strain, *end-1,3(−); Si[end-1(MED-)]; Si[end-3(MED-)]*

that we will refer to as *end-1,3(MED-)*. We observed gut in 75% (n=459) of *end-1,3(MED-)* embryos (Table 1 and Fig. 3B). This is within the range of 50%-85% previously reported for *med-1,2(−)* and *med-1,2(RNAi)* embryos (Goszczynski and McGhee, 2005; Maduro et al., 2007; Maduro et al., 2001), consistent with a partial requirement of the MEDs for endoderm specification.

In using *end* transgenes unlinked from the endogenous *end-1* and *end-3* genes, we considered that the presence of the endogenous though non-functional loci might interfere with expression of the single-copy *end-1* and *end-3* transgenes, for example through competition for a limiting factor. To test for such an effect, we crossed the *end* transgenes into a strain carrying *itDf2*, a deficiency that removes the *end*s and several hundred other genes (Zhu et al., 1997). We found that while 100% of *itDf2; Si[end-1(+)]; Si[end-3(+)]* embryos made gut, 75% (n=198) of *itDf2; Si[end-1(MED-)]; Si[end-3(MED-)]* embryos did (Table 1). These results are in agreement with those obtained with the *end-1(ok558) end-3(ok1448)* double mutant background (p=0.96, χ^2 test), suggesting that the endogenous *end* promoters do not interfere with expression of the single-copy transgene *end* genes used here. One corollary of this result is that no other genes deleted by *itDf2* are necessary to specify endoderm, as single-copy transgenes of *end-1* and *end-3* are sufficient to restore gut specification to all embryos. Additionally, as *itDf2* does not modify the amount of partial gut specification seen in the *end-1,3(MED-)* strain, no genes deleted by *itDf2*, apart from *end-1* and *end-3*, appear to make a significant zygotic contribution to gut specification.

We next examined MED site requirements when only one of *end-1* or *end-3* is present. As noted above, an *end-1,3(−); Si[end-1(+)]* strain makes gut ~95% of the time, and an *end-1,3(−); Si[end-3(+)]* strain makes gut 100% of the time (Fig. 3C, D). Mutation of the MED sites when only *end-1* is present (transgene *Si[end-1(MED-)]*) results in 28% of embryos making gut (n=98; Fig. 3E). This is similar to simultaneous mutation of both *med* genes and *end-3*, which we have previously observed to result in gut specification in 37% of embryos (n=258, p=0.11, χ^2 test) (Maduro et al., 2007). When the MED sites are mutated in *end-3* in the absence of *end-1*, to make *end-1,3(−); Si[end-3(MED-)]*, gut is never made (n=93; Fig. 3F), similar to the 3% of embryos we observed to make gut in a *med-1,2(−); end-1(−)* triple mutant (n=121; p=0.26, Fisher's Exact Test). To determine the minimum number of MED sites that would restore *end-3* activation, we examined gut rescuing ability of single-copy *end-3* transgenes in which one, three, or four of the MED sites were mutated. When the fourth site, most proximal to the start of transcription, is mutated, gut is still made 100% of the time (n=253), and when the first three sites are mutated, gut is made ~85% of the time (n=271; Table 1). Hence, even one MED binding site is usually sufficient for *end-3* to specify endoderm in the absence of *end-1*. We previously showed that a multicopy *end-1* "minimal" GFP reporter array requires at least two MED sites for activation (Broitman-Maduro et al., 2005). This suggests that there is at least one other input into *end-3* activation in addition to the MEDs. By itself, this input is not sufficient to activate *end-3* enough to specify gut when both *end-1* and the MED sites in the *end-3* promoter are absent. Overall, these results show that when a single *end* gene is present, the MED binding sites become important for *end* expression, with *end-3* showing the strongest requirement.

Finally, we tested combinations of *end* transgenes in which one *end* gene carries MED sites and the other does not. Both cases, *end-1,3(−); Si[end-1(MED-)]; Si[end-3(+)]* and *end-1,3(−); Si[end-1(+)]; Si[end-3(MED-)]*, exhibited 100% specification of gut (Table 1).

POP-1 and PAL-1 become necessary for E specification when MED sites are mutated

The existence of parallel inputs into *end* activation is supported by the observation that gut specification occurred in 75% of embryos when the MED binding sites were mutated in both *end-1* and *end-3*. Consistent with this observation, the *end* promoters contain binding sites for the maternal factors SKN-1, POP-1 and PAL-1 (Fig. 2, Table S1) (Bhambhani et al., 2014; Blackwell et al., 1994; Korswagen et al., 2000; Lei et al., 2009). Of these, SKN-1 accounts for the majority of input into *end* activation, as loss of *skn-1* activity results in a failure of gut specification in 65–80% of embryos (Bowerman et al., 1992; Huang et al., 2007; Maduro et al., 2005b). Unlike *skn-1*, loss of *pop-1* or *pal-1* does not exhibit a significant loss of endoderm specification (Hunter and Kenyon, 1996; Lin et al., 1995; Maduro et al., 2005b). Rather, input by POP-1 and PAL-1 can be inferred genetically by enhancement of a background in which *skn-1* is reduced or absent, as simultaneous depletion of *skn-1* with *pop-1* and/or *pal-1* greatly increases the severity of the endoderm specification defect over loss of *skn-1* alone (Huang et al., 2007; Maduro et al., 2007). This is consistent with a model in which SKN-1 provides the major input while POP-1 and PAL-1 provide parallel inputs.

We tested the contributions of SKN-1, POP-1 and PAL-1 in the absence of MED sites by depleting them individually by bacteria-mediated RNAi (Kamath and Ahringer, 2003) in the control and *end-1,3(MED-)* strains. RNAi of *skn-1* in the control strain resulted in specification of gut 30% of the time (n=454), similar to *skn-1(RNAi)* of N2 (Maduro et al., 2005a), while *skn-1(RNAi)* in the *end-1,3(MED-)* strain resulted in gut in 21% of embryos (n=522; $p<0.002$) (Fig. 4A, 4B and Table 2). A similar synergistic effect of genetic loss of *med-1,2(−)* on *skn-1(RNAi)* was also observed in a previous report (Maduro et al., 2007), suggesting that there is some MED activity that is independent of SKN-1, or that *skn-1(RNAi)* does not fully eliminate all *med-1,2* expression. The report of 19% gut made by the progeny of mothers homozygous for the putative null mutation *skn-1(zu67)* 25°C is consistent with the latter (Bowerman et al., 1992). Either way, as ~20% of embryos lacking both SKN-1 and MED-1,2 regulatory input still make endoderm, this must be the result of parallel inputs.

The TCF factor POP-1 has a dual role in E specification: It represses *end-1* and *end-3* in the MS cell, and contributes to Wnt-dependent activation of *end-1* (and possibly *end-3*) in parallel with SKN-1/MED-1,2 (Lin et al., 1995; Owraghi et al., 2010; Shetty et al., 2005). While POP-1-dependent repression of the *end*s occurs via POP-1 sites (alone), POP-1-dependent activation requires the nearby presence of conserved ‘Helper’ sites through which the POP-1/SYS-1 complex likely binds (Bhambhani et al., 2014; Robertson et al., 2014; Shetty et al., 2005). The *end-1* promoter contains a nearby POP-1+Helper site (Fig. 2 and Table S1), and these sites mediate a positive contribution of POP-1 to *end-1* activation (Bhambhani et al., 2014; Shetty et al., 2005). In contrast, the *end-3* promoter has POP-1 sites and putative Helper sites, though the best consensus Helper sites are not near the POP-1

sites (Fig. 2 and Table S1) (Robertson et al., 2014). To test the importance of POP-1 in E specification in the absence of the MED binding sites, we depleted *pop-1* by RNAi in control strains and those with various *end-1* or *end-3* transgenes (Table 2). While *pop-1(RNAi)* of the control strain resulted in endoderm 100% of the time (n=564; Fig. 4C), *pop-1(RNAi)* in the *end-1,3(MED-)* strain resulted in a failure of gut to be specified in all embryos (n=319, p<0.0001; Fig. 4D). Depletion of *pop-1* in other strains showed that compromising MED sites in *end-3* alone, with or without *end-1* present, also results in a complete loss of gut (Table 2). An interesting result is evident in the strain in which *end-1* is absent, but in which *end-3* is present with a single MED binding site, strain *end-1,3(−); Si[end-3(1-2-3-4+)]*: Without *pop-1(RNAi)*, this strain makes gut 85% of the time (n=271, Table 1), but with *pop-1(RNAi)*, gut specification occurs in 1% of embryos (n=345; p<0.0001). This shows that when only *end-3* is present, and its promoter retains only a single MED binding site, a positive contribution from POP-1 becomes nearly essential. These results suggest that in the absence of MED binding sites, POP-1/SYS-1 make a stronger contribution to gut specification than SKN-1.

The Caudal-like regulator PAL-1 is essential for specification of the C and D blastomeres (Hunter and Kenyon, 1996). PAL-1 protein is present in E, and may be more stable than SKN-1, as PAL-1 is detectable in E and its daughters Ea and Ep, while SKN-1 becomes undetectable after E has divided (Bowerman et al., 1993; Hunter and Kenyon, 1996). We have previously shown that in strains partially compromised for endoderm specification, simultaneous depletion of *pal-1* results in a further loss of gut (Maduro et al., 2007). Consistent with direct regulation of *end-1* by PAL-1, the *end-1* promoter contains a single PAL-1 binding site (Fig. 2A and Table S1) (Lei et al., 2009). The *end-3* promoter contains a site that matches the optimal PAL-1 binding site in 8 of 9 base pairs and includes the Caudal binding site (Fig. 2A). We hypothesized that in the absence of the MED binding sites, it should be possible to detect PAL-1-dependent input into endoderm specification with *pal-1(RNAi)*. Consistent with this prediction, while depletion of *pal-1* by RNAi in the control strain resulted in 100% gut specification (n=400; Fig. 4E), *pal-1(RNAi)* in the strain lacking MED sites in *end-1* and *end-3* specified gut only 3% of the time (n=755, p<0.0001; Fig. 4F, Table 2). These results confirm that PAL-1 contributes to E specification in parallel with MED-1,2.

To confirm that the RNA interference results were not dependent on bacteria-mediated RNAi, we injected dsRNA for *skn-1*, *pal-1* and *pop-1* directly into the *end-1,3(MED-)* strain. As shown in Table 2, results were similar for *skn-1(RNAi)* [21% *vs.* 27% with gut] and *pal-1(RNAi)* [3% *vs.* 1%], but we still observed 5% of embryos making gut with *pop-1(RNAi)*. Hence, we conclude that when the MED sites are absent from *end-1* and *end-3*, endoderm specification becomes more dependent on POP-1 and PAL-1 than SKN-1.

The E cell frequently generates an abnormal number of gut nuclei when MED sites are mutated

In wild-type embryos, the E cell generates 20 intestinal cells (Sulston et al., 1983). We have previously reported that in *med-1,2(−)* embryos that contain gut, the number of gut cells varies from 0 to more than 30 (Maduro et al., 2007). This could be due to the failure of all

med-1,2(−) embryos to specify MS, which results in an embryonic arrest at 1- to 1.5-fold elongation (Maduro et al., 2001), or it could be caused by changes in *end-1* and *end-3* activation resulting from loss of MED-1,2 input. To distinguish these possibilities, we examined the generation of gut cells using an integrated *elt-2*::GFP reporter (Fukushige et al., 1998), reasoning that the strains generated here specifically affect only the ability of the MEDs to activate *end-1* and *end-3*, creating the equivalent of a *med-1,2(−)* phenotype that is restricted to the E lineage.

We scored the number of *elt-2*::GFP nuclei in late-stage embryos as shown in Fig. 5A. We first examined the *end-1,3(−); Si[end-1(+)]* strain. As expected, controls exhibited the wild-type number (range of 19–21, $\bar{x}$=20.0±0.1, n=34). Among embryos with gut, the numbers of *elt-2*::GFP nuclei varied from 3–30 in the *end-1,3(−); Si[end-1(+)]* strain, though with a mean similar to the control ($\bar{x}$=19.7±5.7, n=49). This is expected, as this strain should behave similarly to the single *end-3(ok1448)* mutant, which we previously reported to form aberrant numbers of *elt-2*::GFP nuclei (Maduro et al., 2007).

We next evaluated *elt-2*::GFP in *end-1,3(MED-)* embryos. As predicted by the *med-1,2(−)* phenotype, we observed variations in the number of *elt-2*::GFP nuclei among embryos with gut ($\bar{x}$=12.9±0.8, n=85). Overall, 93% of embryos had a non-wild-type number of *elt-2*-expressing cells, which is consistent with the 93–95% of *med-1,2(−)* embryos that fail to generate 20 *elt-2*::GFP nuclei (Maduro et al., 2007). Hence, the aberrant numbers of gut cells seen in terminal *med-1,2(−)* embryos can be attributed to a failure of MED-1,2 to provide input into *end-1* and *end-3*, and not because specification of MS, and overall morphogenesis, also fail to occur.

In the aforementioned strains experiencing partial gut specification, a more severe inability to specify gut appears to predict a greater likelihood of aberrant numbers of *elt-2*::GFP(+) nuclei. To test whether this correlation persists when the proportion of embryos producing gut is extremely low, we examined *elt-2*::GFP in the *end-1,3(−); Si[end-1(MED-)]* strain, which produced gut in 28% of embryos. Many of these embryos have relatively small patches of gut granule-like material (e.g. compare Figs. 3C and 3E). Consistent with this, the numbers of *elt-2*::GFP nuclei among embryos with gut were generally low, with a range of 1–23 nuclei ($\bar{x}$=7.3±0.6, n=79). We conclude that a reduced likelihood of gut specification results in fewer embryos producing gut, and also fewer *elt-2(+)* nuclei when gut is made. This provides strong evidence that gut specification cannot be described as an “all-or-none” phenomenon when regulation of *end-1* and/or *end-3* is partially compromised.

Intestine fate becomes stochastic within the E lineage in *end-1,3* hypomorphic embryos

The basis for the aberrant numbers of gut nuclei in specification-compromised strains could be the result of changes in the division pattern of the E lineage, i.e. the E cell divides too few or too many times, or it may be that in some embryos, E generates a mixture of gut and non-gut cells. Several lines of evidence argue for both as contributing factors. First, the appearance of *elt-2*::GFP nuclei in late-stage embryos is similar in size to controls, and not to the nuclei of early-stage embryos, which are much larger (Fig. 5B–D and data not shown). Second, the *elt-2*::GFP(+) nuclei often appear in different positions in the embryo, suggesting that cells with distinct origins within the E lineage have separately adopted a gut

fate. For example, an arrested larva with five *elt-2*::GFP nuclei (Fig. 5C) contains a cluster of four *elt-2*::GFP nuclei in the anterior and a single such nucleus in the posterior. Hence, when there are much fewer than 20 gut cells in an embryo, this may result from the acquisition of an intestine fate from only some of the descendants of E, and not all of them.

A failure of late-stage embryos to show an intestine identity among all E descendants could occur in one of two ways. The early E lineage cells could always acquire an intestine progenitor identity, but some of them lose this identity over time and adopt an alternate fate; alternatively, acquisition of an intestine fate may occur later within the E lineage. To distinguish these possibilities, we examined fixed time points of control and *end-1,3(MED-)* embryos for their expression of *elt-2*::GFP. Whereas controls exhibited expression appropriate to embryonic stage, many *end-1,3(MED-)* embryos had fewer or no *elt-2*::GFP expressing cells compared to controls (Fig. 5E). We have also examined individual embryos over time, and found that a majority exhibit delayed and weaker onset of *elt-2*::GFP expression, and when *elt-2*::GFP expression was observed, it persisted in the descendants of the expressing cells (HC and MM, data not shown; a more detailed analysis will be presented elsewhere). These results suggest that activation of *elt-2* and commitment to an E fate become delayed and stochastic within the E lineage when *end-1* and *end-3* lack MED binding sites.

Adults derived from surviving *end-1,3(MED-)* transgenic embryos exhibit pleiotropic defects

The current model for gut specification is that *elt-2* activation, reinforced by *elt-7*, determines intestinal fate which is then maintained via positive autoregulation for the life of the animal (Fukushige et al., 1999; McGhee et al., 2009; Sommermann et al., 2010). An important unanswered question is whether endoderm differentiation is robust to delayed activation of *elt-2*: After expression of *end-1* and *end-3* has disappeared, does ELT-2 always drive a normal program of intestinal differentiation?

To examine this question, we examined adults of the *end-1,3(MED-)* and *end-1,3(−); Si[end-1(MED-)]* strains, as these represent mild and severe effects on specification, respectively (Fig. 5), but they also produce some embryos that survive to become fertile adults. As summarized in Fig. 6, many surviving adults exhibited a variety of phenotypes including a short body size (Dpy), egg laying inability (Egl) and sterility (Ste), often along with other morphological defects that were not seen in control animals (Fig. 6A). The defects occurred more frequently in the *end-1,3(−); Si[end-1(MED-)]* surviving adults than *end-1,3(MED-)*, suggesting that the occurrence of the defects correlates with the severity of the embryonic gut specification defect.

Most *end-1,3(MED-)* embryos exhibited aberrant numbers of gut nuclei, including some with many more than the wild-type number of 20 (Fig. 5A). We hypothesized that variability in gut nucleus number might also be observable in adults. To test this, we examined control and *end-1,3(MED-)* L4 animals carrying a *pept-1*::mCherry::H2B reporter. As shown in Fig. 6D, in the control strain we counted a mean of 33.9 ± 0.2 gut nuclei with a range of 32–38 (n=29). This is consistent with the expected number of 34 in adults, as 14 of the 20 L1 gut nuclei undergo a further division prior to the L2 stage (Sulston and Horvitz,

1977). The *end-1,3(MED-)* strain showed a mean of 38.9 ± 0.3 gut nuclei with a range of 31–55 (n=50; $p<10^{-6}$). Hence, adult survivors of this strain display aberrant numbers of gut nuclei with an average increase of approximately five nuclei over the control. We note that no animals were found with fewer than 30 gut nuclei, suggesting that larvae with less than the wild-type number of 20 do not survive to adulthood.

As egg-laying defects and sterility are induced when normal animals are deprived of food (Seidel and Kimble, 2011), we hypothesized that the aforementioned suite of defects results from a defective ability of the intestine to provide adequate nutrition to the animal, resulting in a developmentally-induced caloric restriction (CR). Consistent with this, preliminary data suggest that the *end-1,3* "hypomorphic" adults exhibit abnormally high lipid stores as stained by Oil Red O, even among adults with apparently normal morphology, and despite being fed *ad libitum* (GBM and MM, unpublished observations). Increased lipid stores have been observed in adult *C. elegans* following CR during larval development (Palgunow et al., 2012). In that study, animals given lower amounts of *E. coli* during larval development also exhibited a developmental delay of 4–6 h between embryogenesis and adulthood. To test for a possible developmental delay, we timed development of control and *end-1,3(MED-)* animals to adulthood. While control animals progressed to young adulthood over an average of 49.1 ± 0.1 h (n=130), surviving *end-1,3(MED-)* adults took an average of 54.6 ± 0.3 h (n=90; $p<10^{-37}$), representing a delay of ~ 5.5 h, similar to the delay seen in wild-type animals subjected to larval CR (Palgunow et al., 2012).

Finally, to be sure that these defects are not peculiar to the arrangement of transgenes that we have used here, we examined surviving adults of *med-1(ok804); end-3(ok1448)* double mutants, which make gut 42% of the time, and *end-3(ok1448)* and *end-3(zu247)* single mutants, which each make gut ~95% of the time (Maduro et al., 2007). We observed similar adult phenotypes in both cases, though at a lower frequency in the *end-3* single mutants (data not shown). Hence, the more compromised endoderm specification is overall, the more likely that surviving adults will exhibit defects. These results suggest that a failure to activate endoderm specification in a timely manner causes defects in intestinal differentiation.

Discussion

Specification of the endoderm in *C. elegans* has been a useful model to study how a gene regulatory network directs cell type identity, starting with maternal factors through to terminal regulators (Maduro, 2008). Prior analyses have revealed that specification results from the parallel activities of multiple factors that impinge on activation of *end-1* and *end-3* (Bowerman et al., 1992; Lin et al., 1995; Maduro et al., 2005a; Maduro et al., 2005b; Shetty et al., 2005). Here we have further elucidated the contribution of the divergent GATA factors MED-1 and MED-2 to specification of endoderm, by mutating their binding sites in single-copy transgenes of *end-1* and *end-3* and inserting these into an *end-1 end-3* double-mutant background. We have found that loss of MED-1,2-dependent input into the *end* genes results in delayed *elt-2* activation, lineage defects in embryos, and phenotypes in surviving adults that are suggestive of defects in intestine function. We conclude from these

results that MED-1 and MED-2 promote robust activation of *end-1* and *end-3*, and hence of *elt-2*, to promote proper intestinal specification and differentiation.

POP-1 and PAL-1 function in parallel to SKN-1/MED-1,2 in endoderm specification

Building on prior work establishing input of POP-1 and PAL-1 in E specification in parallel with SKN-1 (Maduro et al., 2005b; Shetty et al., 2005), we have provided additional evidence that SKN-1, POP-1 and PAL-1 together account for endoderm specification that occurs in the absence of the MED binding sites, and shown that the relative contributions of these factors are different. In otherwise wild-type embryos, Wnt-signaled POP-1 and Caudal/PAL-1 are individually dispensable for endoderm specification (Table 2) (Hunter and Kenyon, 1996; Lin et al., 1995). The *end-1,3(MED-)* strain is a compromised background in which regulatory input from POP-1 and PAL-1 both become nearly essential for endoderm to be specified (Table 2). The positive contribution of POP-1 to *end-1* activation requires POP-1 Helper sites in the *end-1* promoter (Bhambhani et al., 2014; Shetty et al., 2005). While the *end-3* promoter contains POP-1 sites, the only nearby sequences to these are not a perfect match to the consensus Helper site (Fig. 2 and Table S1) (Robertson et al., 2014). Here we have found evidence that POP-1 may nonetheless act positively on *end-3*, as *pop-1(RNAi)* can enhance the gut specification defect of an *end-1,3(−)* strain carrying only the *end-3* transgene with a single MED site, in strain *end-1,3(−); Si[end-3(1-2-3-4+)]* (Tables 1 and 2): With no RNAi treatment, this strain makes gut in ~85% of embryos (n=271), while *pop-1(RNAi)* reduces this to ~1% (n=345).

Our results confirm that Caudal/PAL-1, which specifies the C and D fates, contributes to E specification as we reported previously (Maduro et al., 2005b). The positive role of PAL-1 in endoderm is now supported by multiple lines of evidence, including the presence of PAL-1 protein in the early E lineage (Hunter and Kenyon, 1996), the presence of an optimal binding site for PAL-1 in the *end-1* promoter (Fig. 2A), the ability of *pal-1* knockdown to enhance gutlessness in *skn-1(RNAi)* and *end-3* mutants (Maduro et al., 2005b), and the enhancement of the gut specification phenotype of the *end-1,3(MED-)* and similar strains by *pal-1(RNAi)* (this work). Our results suggest that, like POP-1, PAL-1 acts primarily through *end-1*.

Together, POP-1 and PAL-1 provide regulatory input in parallel with SKN-1/MED-1,2. The gut defect of *skn-1(RNAi)* was enhanced only slightly when MED sites were deleted, as the proportion of embryos making gut went from 30% in *skn-1(RNAi)* in the control strain to 21% in the *end-1,3(MED-)* strain (Fig. 4A,B; Table 2); however this may be attributable to an inability of RNAi to completely eliminate endogenous *skn-1* mRNA. The results are nonetheless consistent with the fact that loss of SKN-1 is essential for expression of *med-1* and *med-2* (Maduro et al., 2001). We previously observed that knockdown of both *pop-1* and *pal-1* together by gonadal injection of dsRNA still resulted in specification of gut in all progeny embryos (Maduro et al., 2005b), which suggests that while POP-1 and PAL-1 work in parallel with SKN-1/MED-1,2-dependent activation, they do not synergize with each other. One interpretation of this is that POP-1 and PAL-1 may work cooperatively, as may be the case in the C lineage during muscle specification (Fukushige and Krause, 2005).

Robustness of E specification requires MED-1,2

Our analysis of *end-1,3(MED-)* embryos found that among embryos containing gut, the number of *elt-2*::GFP nuclei frequently deviated from the 20 expected in the wild type. Observation of developing embryos showed that that onset of *elt-2* expression, and hence commitment to intestinal fate, was delayed in many embryos (Fig. 5). As expression of *end-1* and *end-3* reporters became weakened in *med-1,2(−)* embryos (Fig. 1B–E), a reasonable hypothesis is that the amounts of END-1 and END-3 protein made in the absence of MED-1,2 regulatory input are not high enough to robustly activate *elt-2* until the E cell has completed one or more rounds of cell division. In a separate paper, we report that when the MED sites are mutated, the expression levels of *end-3* are curtailed and *end-1* becomes highly variable, leading to delayed and less robust *elt-2* activation (A. C.-Y. W. and S. A. R., in preparation). We can rule out an effect of the single-copy transgenes, as a delay or absence of onset of an integrated *elt-2*::GFP reporter also occurs in *med-1,2(−)* and *med-1(−); end-3(−)* embryos (data not shown). These results are most consistent with a model in which MED-1,2 act on *end-1,3* to assure a timely commitment to an endoderm fate. We have previously observed aberrations in numbers of *elt-2*::GFP nuclei in *skn-1(RNAi), med-1(−); end-3(−)* double mutant and *med-1,2(−)* double mutant embryos, but it was not possible to separate out possible cell non-autonomous effects resulting from loss of MED function in the MS lineage (Maduro et al., 2007). We and others have seen less frequent aberrations in the division pattern of cells in the early E lineage in single *end-3* mutants, but these specify endoderm at a relatively high rate (~95%) and hence onset of *elt-2* expression is likely not as severely affected (Boeck et al., 2011; Maduro et al., 2005a). In other backgrounds, such as gain-of-function mutations in *cdc-25.1*, the E lineage produces supernumerary embryonic nuclei with no other apparent phenotypes (Clucas et al., 2002; Kostic and Roy, 2002), consistent with findings that show that specification and the pattern of cell divisions can be uncoupled (Nair et al., 2013).

If only some cells in the E lineage adopt an intestine fate in hypomorphic specification strains, what happens to those cells that do not? Our prior work has established that when *end-1* and *end-3* are both mutated, E adopts the fate of the C cell and makes mesoderm and ectodermal cells, similar to the fate of the E cell in *skn-1*-depleted embryos that fail to make gut (Bowerman et al., 1992; Maduro et al., 2005a; Owraghi et al., 2010; Zhu et al., 1997). The C fate is specified by Caudal/PAL-1, which is also found in the nucleus of E and its daughters (Hunter and Kenyon, 1996). This suggests that there is potential for non-endoderm E descendants to make C-type tissues (muscle and hypodermis) in at least some *end-1,3(MED-)* embryos that make partial guts. While we did not directly evaluate the fate of presumptive transformed E descendants, we observed ectopic, enclosed hypodermis-lined cavities in some terminal embryos with a partial gut (not shown), similar to structures observed in *end-1,3(−)* embryos (Owraghi et al., 2010) and in embryos lacking *skn-1* or *med-1,2* function (Bowerman et al., 1992; Maduro et al., 2001). Hence, it is likely that the non-endoderm E descendants in hypomorphic gut specification strains adopt fates consistent with the complete absence of *end-1* and *end-3*.

As shown in Fig. 7, we propose that the loss of the MED binding sites makes endoderm specification highly sensitive to stochastic differences in other upstream contributions to

end-1,3 activation, which in turn affects which cells in the E lineage activate *elt-2* to a sufficient degree to commit to an intestine fate. In this model, E specification is still subject to a threshold of [END-1+END-3] activity, but that threshold can no longer be reliably reached within the first few cell cycles of the E lineage when *end-1* and *end-3* lack regulatory input from MED-1,2. This results in a loss of the robustness of intestine precursor specification, which also compromises intestine function as discussed below.

Adults exhibit phenotypes in “hypomorphic specification” strains

Most of the strains in which endoderm specification is compromised are viable as homozygotes, although many *end-1,3(MED-)* and *end-1,3(−); Si[end-1(MED-)]* animals arrest as embryos or L1s, even though they contain some gut cells. As wild-type animals that hatch under starvation conditions arrest development in the L1 stage (Baugh, 2013), survival of hypomorphic gut specification animals to the L2 stage selects for those that have a functional gut. We have found that as adults, these animals may manifest visible defects in egg laying, morphology and sterility (Fig. 6A, C). As these defects are correlated with a developmental delay and an overall increase in gut nucleus number (Fig. 6B, D), it is possible that the presence of excess gut nuclei causes these defects. However, gain-of-function mutations in *cdc-25.1* result in supernumerary gut nuclei without affecting gut specification, and these were not reported to have morphological defects or changes in intestine function (Clucas et al., 2002; Kostic and Roy, 2002). The gut nucleus number defects are also more extreme in the *cdc-25.1(gf)* mutants than we have seen: Whereas surviving adults of the *end-1,3(MED-)* strain have an average of five more nuclei at the L4 stage, *cdc-25.1(gf)* animals have as many as ~25 more (Kostic and Roy, 2002). Instead, these phenotypes may result from abnormal metabolism, as we observed increases in lipid stores and developmental delay, both of which are consistent with caloric restriction (Palgunow et al., 2012).

Our results raise the possibility that adults surviving hypomorphic specification can influence the phenotype of their offspring because they have defects in their intestine. This might occur if these animals inappropriately apportion resources to oocytes, or through an epigenetic mechanism (Rechavi et al., 2014; Seidel and Kimble, 2011). However, all of the transgenic strains we have studied here, including the *end-1,3(MED-)* strain, demonstrated relatively consistent generation-to-generation stability in the proportion of embryos that made gut and in the proportion of adults exhibiting defects. Indeed, we might predict that the healthiest animals would propagate more efficiently to the next generation through a shorter generation time and production of a greater proportion of viable embryos. Consistent with this, when the *end-1,3(MED-)* strain was first generated, we measured a stronger endoderm defect, with 33% of embryos failing to make gut (n=223), which is greater than the 25% seen after several generations (n=459; $p<0.02$). Furthermore, this strain showed the same likelihood of gut specification as homozygous *itDf2; end-1,3(MED-)* embryos segregated from *itDf2/+; end-1,3(MED-)* mothers, which are hemizygous for the wild-type *end-1* and *end-3* genes (Table 1). This suggests that laboratory propagation favors the maintenance of the least affected animals, as opposed to worsening the phenotype over time.

Early specification defects propagate through the endoderm GRN

The current understanding of the *C. elegans* endoderm GRN features transient cell specification factors that ultimately activate a positive feedback of terminal differentiation via *elt-2* (Fig. 1A). The activity of the upstream *end-1* and *end-3* genes is transient and occurs when the embryo has fewer than 100 cells (Maduro et al., 2005a; Zhu et al., 1997). Despite the positive autoregulation of *elt-2* at the end of this network, a small perturbation in activation of *end-1* and *end-3*, through elimination of what has been thought to be only a minor regulatory input, is sufficient to produce a cascade of defects that are visible in surviving adults.

What is the mechanistic basis for the adult gut defects? Although surviving *end-1,3(MED-)* embryos produce a functional gut, they may be deficient in an activity that is required for normal metabolism. As there is no evidence that the *med*s or *end*s are expressed in the adult intestine (McGhee et al., 2007; Pauli et al., 2006), the simplest interpretation is that reduced *end-1* and/or *end-3* activation, as a result of loss of MED-1,2 regulatory input, propagates an effect through the GRN that leads to intestinal differentiation through *elt-2*. Consistent with this, we have observed a delay in the embryonic activation of *elt-2*, the central regulator of intestine fate, in *end-1,3(MED-)* embryos and similar strains that are partially compromised for embryonic gut specification. Although surviving adults have apparently normal expression of an *elt-2*::GFP reporter, it may be that endogenous *elt-2* expression becomes limiting. However, in a preliminary experiment to test this hypothesis, we introduced an additional genomic copy of *elt-2(+)* via MosSCI into the *end-1,3(MED-)* background, but failed to observe an improvement in adult defects (GBM and MM, unpublished observations).

Another explanation for the adult defects might be that delayed onset of *elt-2* expression within the E lineage misses a timely opportunity to activate particular gut differentiation genes. Indeed, the intestinal gene *glo-1* is activated in the E daughter cells and remains on for the lifetime of the animal (Hermann et al., 2005), suggesting its expression is initially activated by END-1,3 and is maintained by ELT-2. Loss of *glo-1* function results in a loss of gut granules (Hermann et al., 2005), but *elt-2*::GFP-expressing cells in *end-1,3(MED-)* animals are always associated with gut granule-like material, suggesting that *glo-1* does eventually become expressed. Nonetheless, it may be that a delay or reduction of expression of genes such as *glo-1* may initiate a cascade of changes in physiology that persist through larval development and into adult.

Regardless of the molecular basis for the effects we have seen, it is unexpected that intestinal gene expression does not become properly remodeled during postembryonic development, long after specification has occurred. One interpretation is that the endoderm GRN has been made robust in its most upstream components, rather than throughout the network. This is consistent with the diverse set of parallel inputs that participate in activation of *end-1* and *end-3*. More generally, we propose that in any metazoan system in which progenitors acquire tissue type identity through such networks, it is possible that “hypomorphic” specification of a cell type results in heterogeneous differentiated states that can directly affect the quality of terminal development. This finding has implications for

other cell specification gene networks in many systems, including the programming of embryonic stem cells.

Supplementary Material

Refer to Web version on PubMed Central for supplementary material.

Acknowledgments

We are grateful to Christian Frokjaer-Jensen and Erik Jorgensen for sending reagents for MosSCI, and for extensive advice; Leila Magistrado, Shruthi Satish and Gurjot Walia (undergraduate students at UC Riverside) for assistance with collection of preliminary data not reported here; Angela Stathopoulos (Caltech, Pasadena, CA) and Chris Hopkins at Knudra (Murray, UT) for helpful discussions; and helpful suggestions from the anonymous reviewers. Some plasmids were obtained from Addgene (Cambridge, MA). F.C. was supported by NIH Award Number T34GM062756 from the National Institute of General Medical Sciences (MARCU-STAR) program to UC Riverside. Some strains were provided by the CGC, which is funded by the NIH Office of Research Infrastructure Programs (P40 OD010440). This work was supported by NSF grants IOS#0643325 and IOS#1258054, and a UCR Committee on Research Award to M.M.; and NIH grant #R01GM103782 to S.R.

References

Bao Z, Murray JI, Boyle T, Ooi SL, Sandel MJ, Waterston RH. Automated cell lineage tracing in Caenorhabditis elegans. Proceedings of the National Academy of Sciences of the United States of America. 2006; 103:2707–2712. [PubMed: 16477039]

Baugh LR. To grow or not to grow: nutritional control of development during Caenorhabditis elegans L1 arrest. Genetics. 2013; 194:539–555. [PubMed: 23824969]

Baugh LR, Hill AA, Slonim DK, Brown EL, Hunter CP. Composition and dynamics of the Caenorhabditis elegans early embryonic transcriptome. Development. 2003; 130:889–900. [PubMed: 12538516]

Bhambhani C, Ravindranath AJ, Mentink RA, Chang MV, Betist MC, Yang YX, Koushika SP, Korswagen HC, Cadigan KM. Distinct DNA binding sites contribute to the TCF transcriptional switch in C. elegans and Drosophila. PLoS genetics. 2014; 10:e1004133. [PubMed: 24516405]

Blackwell TK, Bowerman B, Priess JR, Weintraub H. Formation of a monomeric DNA binding domain by Skn-1 bZIP and homeodomain elements. Science. 1994; 266:621–628. [PubMed: 7939715]

Boeck ME, Boyle T, Bao Z, Murray J, Mericle B, Waterston R. Specific roles for the GATA transcription factors end-1 and end-3 during C. elegans E-lineage development. Developmental biology. 2011; 358:345–355. [PubMed: 21854766]

Bowerman B, Draper BW, Mello CC, Priess JR. The maternal gene skn-1 encodes a protein that is distributed unequally in early C. elegans embryos. Cell. 1993; 74:443–452. [PubMed: 8348611]

Bowerman B, Eaton BA, Priess JR. skn-1, a maternally expressed gene required to specify the fate of ventral blastomeres in the early C. elegans embryo. Cell. 1992; 68:1061–1075. [PubMed: 1547503]

Broitman-Maduro G, Maduro MF, Rothman JH. The noncanonical binding site of the MED-1 GATA factor defines differentially regulated target genes in the C. elegans mesendoderm. Developmental cell. 2005; 8:427–433. [PubMed: 15737937]

Captan VV, Goszczynski B, McGhee JD. Neither maternal nor zygotic med-1/med-2 genes play a major role in specifying the Caenorhabditis elegans endoderm. Genetics. 2007; 175:969–974. [PubMed: 17151237]

Chang W, Lloyd CE, Zarkower D. DSH-2 regulates asymmetric cell division in the early C. elegans somatic gonad. Mechanisms of development. 2005; 122:781–789. [PubMed: 15907376]

Clucas C, Cabello J, Bussing I, Schnabel R, Johnstone IL. Oncogenic potential of a C.elegans cdc25 gene is demonstrated by a gain-of-function allele. The EMBO journal. 2002; 21:665–674. [PubMed: 11847114]

Davidson EH, Levine MS. Properties of developmental gene regulatory networks. Proceedings of the National Academy of Sciences of the United States of America. 2008; 105:20063–20066. [PubMed: 19104053]

Frokjaer-Jensen C, Davis MW, Ailion M, Jorgensen EM. Improved Mos1-mediated transgenesis in C. elegans. Nature methods. 2012; 9:117–118. [PubMed: 22290181]

Frokjaer-Jensen C, Davis MW, Hopkins CE, Newman BJ, Thummel JM, Olesen SP, Grunnet M, Jorgensen EM. Single-copy insertion of transgenes in Caenorhabditis elegans. Nature genetics. 2008; 40:1375–1383. [PubMed: 18953339]

Fukushige T, Hawkins MG, McGhee JD. The GATA-factor elt-2 is essential for formation of the Caenorhabditis elegans intestine. Developmental biology. 1998; 198:286–302. [PubMed: 9659934]

Fukushige T, Hendzel MJ, Bazett-Jones DP, McGhee JD. Direct visualization of the elt-2 gut-specific GATA factor binding to a target promoter inside the living Caenorhabditis elegans embryo. Proceedings of the National Academy of Sciences of the United States of America. 1999; 96:11883–11888. [PubMed: 10518545]

Fukushige T, Krause M. The myogenic potency of HLH-1 reveals wide-spread developmental plasticity in early C. elegans embryos. Development. 2005; 132:1795–1805. [PubMed: 15772130]

Goszczynski B, McGhee JD. Re-evaluation of the role of the med-1 and med-2 genes in specifying the C. elegans endoderm. Genetics. 2005

Grishkevich V, Hashimshony T, Yanai I. Core promoter T-blocks correlate with gene expression levels in C. elegans. Genome research. 2011; 21:707–717. [PubMed: 21367940]

Hao Y, Hu Z, Sieburth D, Kaplan JM. RIC-7 promotes neuropeptide secretion. PLoS genetics. 2012; 8:e1002464. [PubMed: 22275875]

Hermann GJ, Schroeder LK, Hieb CA, Kershner AM, Rabbitts BM, Fonarev P, Grant BD, Priess JR. Genetic analysis of lysosomal trafficking in Caenorhabditis elegans. Molecular biology of the cell. 2005; 16:3273–3288. [PubMed: 15843430]

Huang S, Shetty P, Robertson SM, Lin R. Binary cell fate specification during C. elegans embryogenesis driven by reiterated reciprocal asymmetry of TCF POP-1 and its coactivator beta-catenin SYS-1. Development. 2007; 134:2685–2695. [PubMed: 17567664]

Hunter CP, Kenyon C. Spatial and temporal controls target pal-1 blastomere-specification activity to a single blastomere lineage in C. elegans embryos. Cell. 1996; 87:217–226. [PubMed: 8861906]

Kamath RS, Ahringer J. Genome-wide RNAi screening in Caenorhabditis elegans. Methods. 2003; 30:313–321. [PubMed: 12828945]

Kamath RS, Martinez-Campos M, Zipperlen P, Fraser AG, Ahringer J. Effectiveness of specific RNA-mediated interference through ingested double-stranded RNA in Caenorhabditis elegans. Genome biology. 2001; 2:RESEARCH0002. [PubMed: 11178279]

Korswagen HC, Herman MA, Clevers HC. Distinct beta-catenins mediate adhesion and signalling functions in C. elegans. Nature. 2000; 406:527–532. [PubMed: 10952315]

Kostic I, Roy R. Organ-specific cell division abnormalities caused by mutation in a general cell cycle regulator in C. elegans. Development. 2002; 129:2155–2165. [PubMed: 11959825]

Lei H, Liu J, Fukushige T, Fire A, Krause M. Caudal-like PAL-1 directly activates the bodywall muscle module regulator hlh-1 in C. elegans to initiate the embryonic muscle gene regulatory network. Development. 2009

Lin R, Hill RJ, Priess JR. POP-1 and anterior-posterior fate decisions in C. elegans embryos. Cell. 1998; 92:229–239. [PubMed: 9458047]

Lin R, Thompson S, Priess JR. pop-1 encodes an HMG box protein required for the specification of a mesoderm precursor in early C. elegans embryos. Cell. 1995; 83:599–609. [PubMed: 7585963]

Lowry JA, Atchley WR. Molecular evolution of the GATA family of transcription factors: conservation within the DNA-binding domain. J Mol Evol. 2000; 50:103–115. [PubMed: 10684344]

Lowry JA, Gamsjaeger R, Thong SY, Hung W, Kwan AH, Broitman-Maduro G, Matthews JM, Maduro M, Mackay JP. Structural analysis of MED-1 reveals unexpected diversity in the mechanism of DNA recognition by GATA-type zinc finger domains. The Journal of biological chemistry. 2009; 284:5827–5835. [PubMed: 19095651]

Maduro M, Hill RJ, Heid PJ, Newman-Smith ED, Zhu J, Priess J, Rothman J. Genetic redundancy in endoderm specification within the genus Caenorhabditis. Developmental biology. 2005a; 284:509–522. [PubMed: 15979606]

Maduro MF. Structure and evolution of the C. elegans embryonic endomesoderm network. Biochim Biophys Acta. 2008

Maduro MF, Broitman-Maduro G, Mengarelli I, Rothman JH. Maternal deployment of the embryonic SKN-1-->MED-1,2 cell specification pathway in C. elegans. Developmental biology. 2007; 301:590–601. [PubMed: 16979152]

Maduro MF, Kasmir JJ, Zhu J, Rothman JH. The Wnt effector POP-1 and the PAL-1/Caudal homeoprotein collaborate with SKN-1 to activate C. elegans endoderm development. Developmental biology. 2005b; 285:510–523. [PubMed: 16084508]

Maduro MF, Lin R, Rothman JH. Dynamics of a developmental switch: recursive intracellular and intranuclear redistribution of Caenorhabditis elegans POP-1 parallels Wnt-inhibited transcriptional repression. Developmental biology. 2002; 248:128–142. [PubMed: 12142026]

Maduro MF, Meneghini MD, Bowerman B, Broitman-Maduro G, Rothman JH. Restriction of mesendoderm to a single blastomere by the combined action of SKN-1 and a GSK-3beta homolog is mediated by MED-1 and -2 in C. elegans. Mol Cell. 2001; 7:475–485. [PubMed: 11463373]

Maduro MF, Rothman JH. Making worm guts: the gene regulatory network of the Caenorhabditis elegans endoderm. Developmental biology. 2002; 246:68–85. [PubMed: 12027435]

McGhee JD, Fukushige T, Krause MW, Minnema SE, Goszczynski B, Gaudet J, Kohara Y, Bossinger O, Zhao Y, Khattra J, Hirst M, Jones SJ, Marra MA, Ruzanov P, Warner A, Zapf R, Moerman DG, Kalb JM. ELT-2 is the predominant transcription factor controlling differentiation and function of the C. elegans intestine, from embryo to adult. Developmental biology. 2009; 327:551–565. [PubMed: 19111532]

McGhee JD, Sleumer MC, Bilenky M, Wong K, McKay SJ, Goszczynski B, Tian H, Krich ND, Khattra J, Holt RA, Baillie DL, Kohara Y, Marra MA, Jones SJ, Moerman DG, Robertson AG. The ELT-2 GATA-factor and the global regulation of transcription in the C. elegans intestine. Developmental biology. 2007; 302:627–645. [PubMed: 17113066]

Nair G, Walton T, Murray JI, Raj A. Gene transcription is coordinated with, but not dependent on, cell divisions during C. elegans embryonic fate specification. Development. 2013; 140:3385–3394. [PubMed: 23863485]

Nehrke K. A reduction in intestinal cell pHi due to loss of the Caenorhabditis elegans Na+/H+ exchanger NHX-2 increases life span. The Journal of biological chemistry. 2003; 278:44657–44666. [PubMed: 12939266]

Owraghi M, Broitman-Maduro G, Luu T, Roberson H, Maduro MF. Roles of the Wnt effector POP-1/TCF in the C. elegans endomesoderm specification gene network. Developmental biology. 2010; 340:209–221. [PubMed: 19818340]

Palgunow D, Klapper M, Doring F. Dietary restriction during development enlarges intestinal and hypodermal lipid droplets in Caenorhabditis elegans. PloS one. 2012; 7:e46198. [PubMed: 23185233]

Pauli F, Liu Y, Kim YA, Chen PJ, Kim SK. Chromosomal clustering and GATA transcriptional regulation of intestine-expressed genes in C. elegans. Development. 2006; 133:287–295. [PubMed: 16354718]

Phillips BT, Kidd AR 3rd, King R, Hardin J, Kimble J. Reciprocal asymmetry of SYS-1/beta-catenin and POP-1/TCF controls asymmetric divisions in Caenorhabditis elegans. Proceedings of the National Academy of Sciences of the United States of America. 2007; 104:3231–3236. [PubMed: 17296929]

Putzke AP, Rothman JH. Repression of Wnt signaling by a Fer-type nonreceptor tyrosine kinase. Proceedings of the National Academy of Sciences of the United States of America. 2010; 107:16154–16159. [PubMed: 20805471]

Raj A, Rifkin SA, Andersen E, van Oudenaarden A. Variability in gene expression underlies incomplete penetrance. Nature. 2010; 463:913–918. [PubMed: 20164922]

Rechavi O, Houri-Ze'evi L, Anava S, Goh WS, Kerk SY, Hannon GJ, Hobert O. Starvation-induced transgenerational inheritance of small RNAs in C. elegans. Cell. 2014; 158:277–287. [PubMed: 25018105]

Rifkin SA. Identifying fluorescently labeled single molecules in image stacks using machine learning. Methods Mol Biol. 2011; 772:329–348. [PubMed: 22065448]

Robertson SM, Medina J, Lin R. Uncoupling different characteristics of the C. elegans E lineage from differentiation of intestinal markers. PloS one. 2014; 9:e106309. [PubMed: 25181289]

Rocheleau CE, Downs WD, Lin R, Wittmann C, Bei Y, Cha YH, Ali M, Priess JR, Mello CC. Wnt signaling and an APC-related gene specify endoderm in early C. elegans embryos. Cell. 1997; 90:707–716. [PubMed: 9288750]

Seidel HS, Kimble J. The oogenic germline starvation response in C. elegans. PloS one. 2011; 6:e28074. [PubMed: 22164230]

Shetty P, Lo MC, Robertson SM, Lin R. C. elegans TCF protein, POP-1, converts from repressor to activator as a result of Wnt-induced lowering of nuclear levels. Developmental biology. 2005; 285:584–592. [PubMed: 16112103]

Sommermann EM, Strohmaier KR, Maduro MF, Rothman JH. Endoderm development in Caenorhabditis elegans: the synergistic action of ELT-2 and -7 mediates the specification-->differentiation transition. Developmental biology. 2010; 347:154–166. [PubMed: 20807527]

Sulston JE, Horvitz HR. Post-embryonic cell lineages of the nematode, Caenorhabditis elegans. Developmental biology. 1977; 56:110–156. [PubMed: 838129]

Sulston JE, Schierenberg E, White JG, Thomson JN. The embryonic cell lineage of the nematode Caenorhabditis elegans. Developmental biology. 1983; 100:64–119. [PubMed: 6684600]

Thorpe CJ, Schlesinger A, Carter JC, Bowerman B. Wnt signaling polarizes an early C. elegans blastomere to distinguish endoderm from mesoderm. Cell. 1997; 90:695–705. [PubMed: 9288749]

Wu AC, Rifkin SA. Aro: a machine learning approach to identifying single molecules and estimating classification error in fluorescence microscopy images. BMC bioinformatics. 2015; 16:102. [PubMed: 25880543]

Zhu J, Hill RJ, Heid PJ, Fukuyama M, Sugimoto A, Priess JR, Rothman JH. end-1 encodes an apparent GATA factor that specifies the endoderm precursor in Caenorhabditis elegans embryos. Genes & development. 1997; 11:2883–2896. [PubMed: 9353257]

Highlights

- Loss of MED-1,2 binding sites in *end-1,3* results in variable gut abnormalities
- Acquisition of intestinal fate is not an all-or-none event
- Hypomorphic gut specification causes adult defects similar to caloric restriction
- Defects in early specification can manifest through differentiation

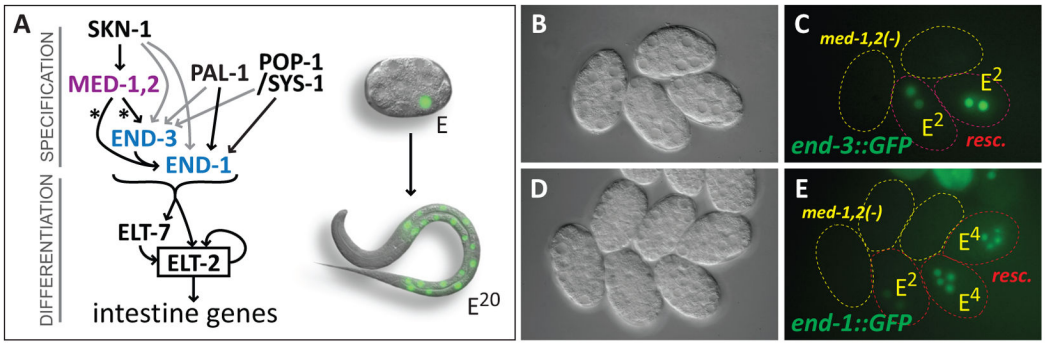

Fig. 1.

Endoderm specification pathway in *C. elegans* and requirement of MED-1,2 for high levels of *end-1* and *end-3* reporter expression. (A) Gene Regulatory Network for specification of E showing convergent upstream inputs of SKN-1, POP-1/SYS-1, and PAL-1 (Maduro, 2008). SKN-1 is a bZIP/Homeodomain factor (Blackwell et al., 1994), POP-1 is the TCF-like *C. elegans* Wnt effector (Lin et al., 1998), and PAL-1 is a Caudal-like homeodomain protein (Hunter and Kenyon, 1996). All of *med-1*, *med-2*, *end-1*, *end-3*, *elt-7* and *elt-2* encode C4 zinc finger GATA type transcription factors, although MED-1 and MED-2 belong to a divergent novel subclass with a unique binding site (Lowry and Atchley, 2000; Lowry et al., 2009). On the right, a 12-cell embryo is shown with the E nucleus showing GFP fluorescence, above a newly-hatched L1 larva (approximately to scale) showing the nuclei of the 20 E descendants in the intestine. The embryo and larva images are from a previous work (Maduro and Rothman, 2002). (B,C) Expression of an integrated *end-3*::GFP reporter (*wIs137*) in rescued and non-rescued *med-1(ok804); med-2(cxTi9744)* embryos. Rescued embryos carry the free duplication *irDp1*, which rescues *med-1,2(−)* lethality and whose presence was ascertained by expression of an *unc-119*::YFP reporter on *irDp1* at a later time point (Maduro et al., 2007). (D,E) Expression of an integrated *end-1*::GFP::H2B reporter (*teIs46*) (Shetty et al., 2005) in the same *med-1,2(−); irDp1* strain. In panels C and E, embryos carrying *irDp1* are outlined in red, while those lacking *irDp1* are outlined in yellow. A *C. elegans* embryo is approximately 50μm long.

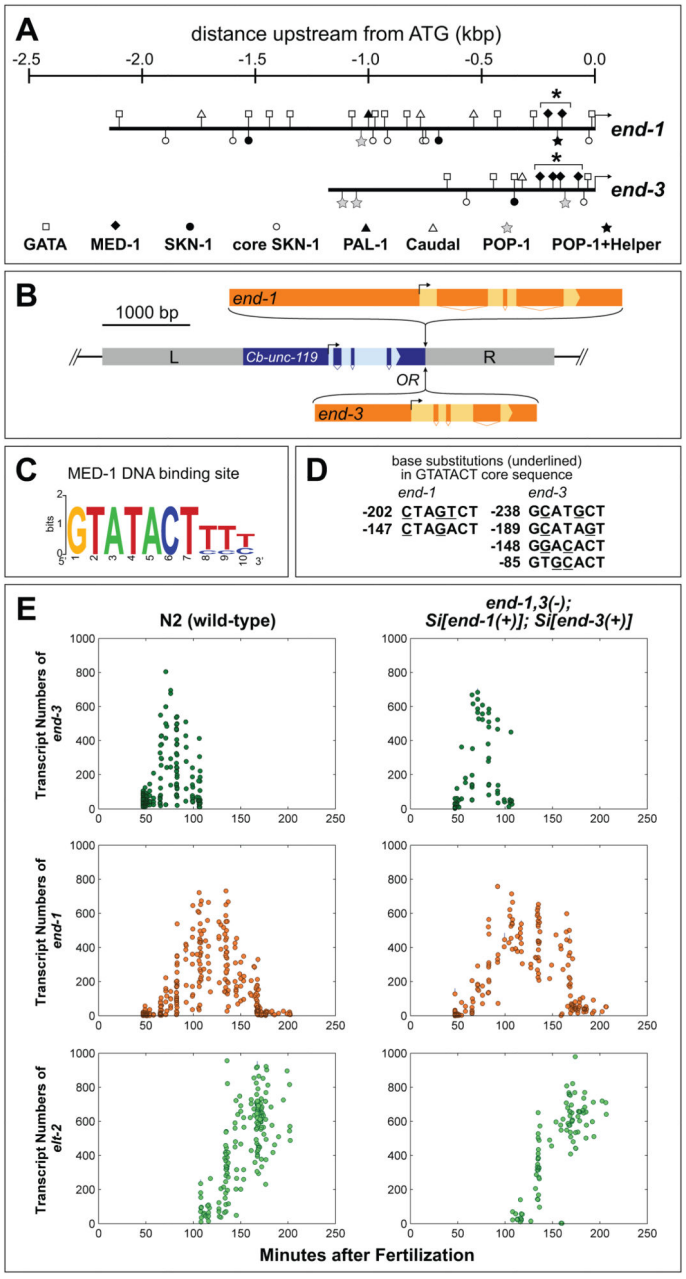

Fig. 2.

Construction of wild-type and MED-site mutated *end-1* and *end-3* single-copy transgenes. (A) Promoter structure of the *end-1* and *end-3* genes. The complete 5′ region up to the coding region of the nearest upstream gene is taken to be the 5′ end of the promoters. Putative binding sites for GATA factors (presumptive sites for END-1 and/or END-3), MED-1, SKN-1 and POP-1 are shown as described in Table S1. The cluster of MED-1 binding sites in each gene is indicated by an asterisk (*). The proximal POP-1 site in *end-1* is adjacent to Helper sequences (Bhambhani et al., 2014). (B) General structure of MosSCI-mediated targeting constructs. Either *end-1* or *end-3* were inserted downstream of *Cb-unc-119(+)* in a vector to target the Mos insertion site in *ttTi5605 II* (for *end-1*) or *ttTi4348 I*

(for *end-3*); homology arms (L and R) were appropriate to the insertion site. These insertion sites have been previously found to be compatible with normal expression of other transgenes, including those that are maternally expressed (Frokjaer-Jensen et al., 2012). (C) Structure of the MED-1 binding sites (Lowry et al., 2009). (D) Mutations introduced at the MED binding sites in *end-1* or *end-3*. At least two base pairs were mutated within the GTATACT invariant core. The location of each site is given in bp relative to the ATG start codon. The mutations do not alter any other known binding sites, including those of the POP-1 Helper sequences (Bhambhani et al., 2014) or of a putative TATA box, as the MED site differs from the TATA consensus (Grishkevich et al., 2011; Lowry et al., 2009). (E) Expression levels in transcripts per embryo of *end-3, end-1* and *elt-2*. Each dot represents a single embryo. Lines across each dot represent a 95% confidence interval for the expression level of that embryo. Minutes after fertilization is based on mapping to nuclei count to time at 25°C using data from a prior report (Bao et al., 2006).

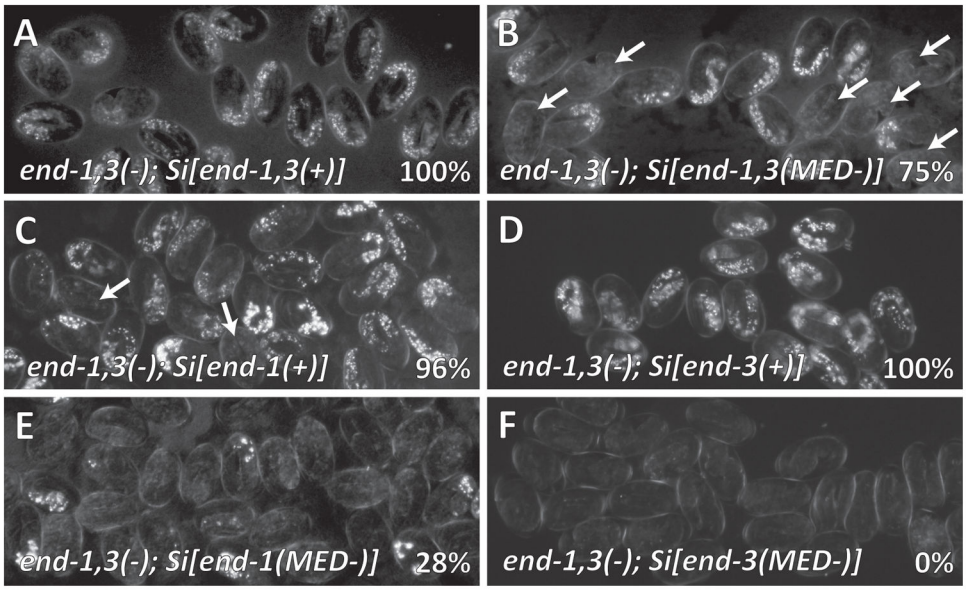

Fig. 3.

Polarized light micrographs showing gut granules in *end-1(ok558) end-3(ok1448)* double mutants transgenic for single-copy insertions of *end* transgenes. Percentages indicate proportion of embryos containing gut. (A) Control (wild-type) *Si[end-1(+)]* and *Si[end-3(+)]*. (B) Single-copy *end-1* and *end-3* transgenes in which all MED binding sites were mutated, *end-1,3(−); Si[end-1(MED-)]; Si[end-3(MED-)]*, a strain referred to as *end-1,3(MED-)* in the text. (C) *Si[end-1(+)]* alone. In panels B and C, some embryos lacking gut are indicated with arrows. (D) *Si[end-3(+)]* alone. (E) *Si[end-1(MED-)]* alone. Very few embryos contain gut granules. (F) *Si[end-3(MED-)]* alone, in which no embryos contain endoderm.

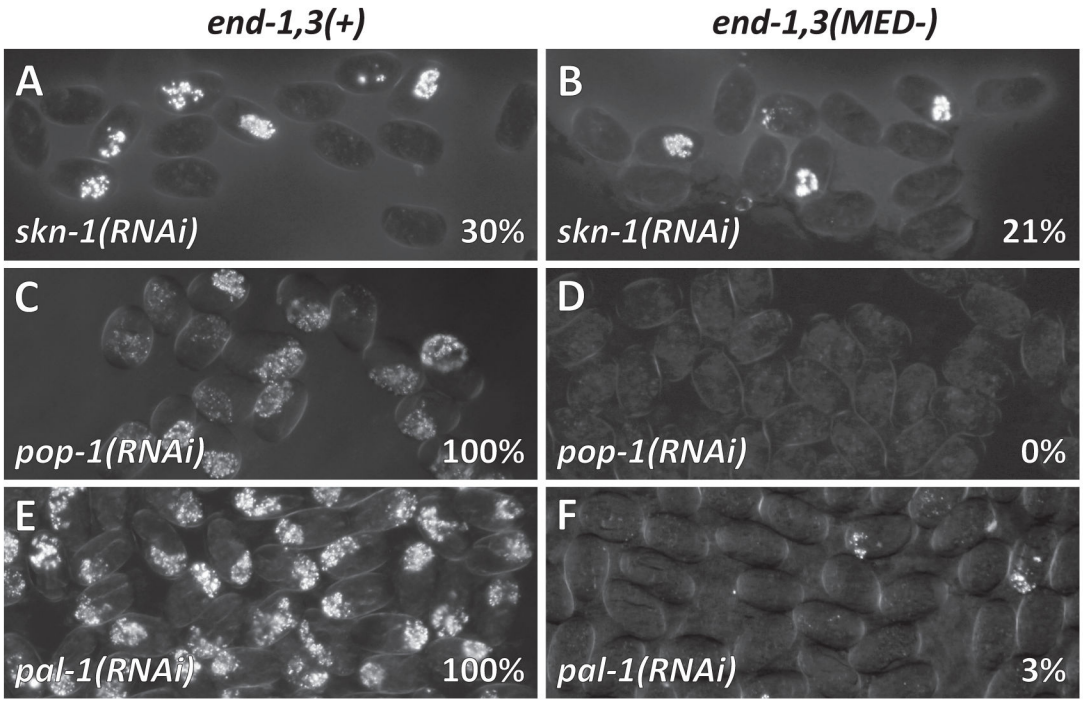

Fig. 4.

Synergistic loss of endoderm occurs in bacterial feeding-based RNAi targeting *skn-1*, *pop-1* or *pal-1* in *end-1,3(−)* embryos transgenic for *end* transgenes. Percentages indicate proportion of embryos containing gut. Left column: Control *Si[end-1(+)]* and *Si[end-3(+)]* transgenes in an *end-1,3(−)* background. Right column: *Si[end-1(MED-)* and *Si[end-3(MED-)]* transgenes in an *end-1,3(−)* background.

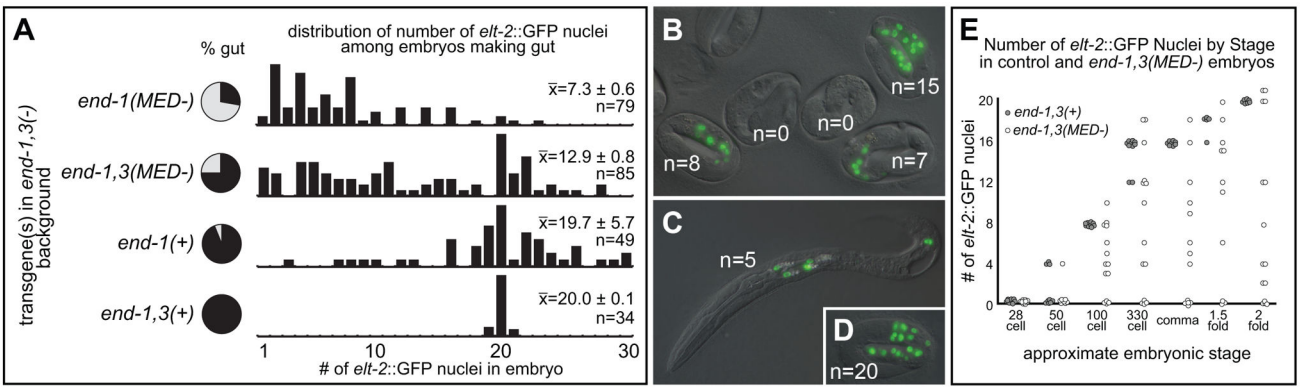

Fig. 5.

Number of gut nuclei becomes highly variable when gut specification is partially compromised. (A) Histograms showing relative number of embryos with amount of *elt-2*::GFP nuclei as indicated along the bottommost X-axis; only embryos containing at least one *elt-2*::GFP nucleus are included. The relative bar heights are scaled to the highest numeric class for each case. To the left of the histograms, a pie chart shows the proportion embryos containing gut without regard to number of gut nuclei. The reporter itself does not cause the changes in gut nuclei, as similar strains lacking the reporter still exhibit patches of gut granules (e.g. many embryos Fig. 3E), and we were able to see similar effects on number of nuclei expressing an integrated *pept-1*::mCherry reporter (not shown). (B–D) DIC micrographs digitally overlaid with GFP fluorescence. (B) Example of late-stage *end-1,3(MED-)* embryos with no gut and variable amounts of gut nuclei shown by *elt-2*::GFP expression. (C) A terminal L1 larva showing four nuclei in the anterior and one in the posterior. Note presence of gut granules (white speckles) around these nuclei. (D) Appearance of *elt-2*::GFP in a late-stage control embryo. (E) Number of *elt-2*::GFP-expressing nuclei at various stages during embryonic development, comparing the control strain (solid circles) with the *end-1,3(MED-)* strain (open circles).

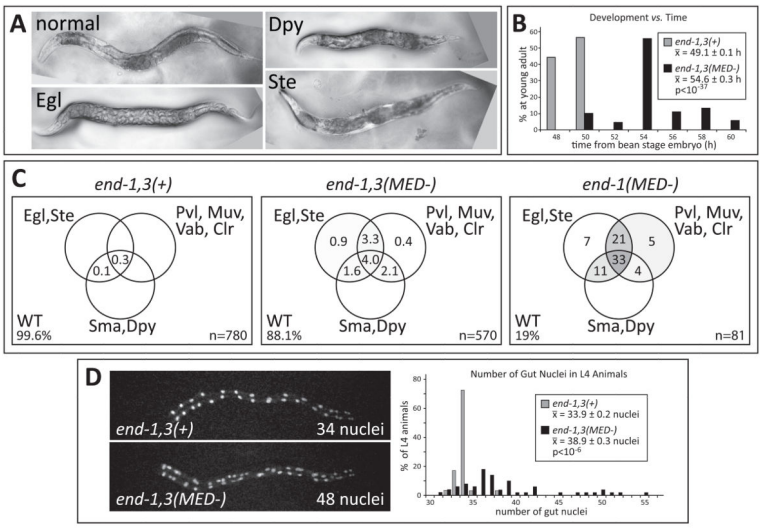

Fig. 6.

Post-embryonic defects are apparent in specification-compromised strains. (A) Phase-contrast images of adults on plates. (B) Bar chart showing that relative to controls, surviving adults of the *end-1,3(MED-)* strain experience an average developmental delay of 5.5 h during larval development. 134 control and 90 *end-1,3(MED-)* animals were scored. (C) Venn diagrams showing appearance of phenotypes as a percentage of total number of adults scored. Within the circles, regions are shaded gray in proportion to the percentage. Egl = egg laying defective; Ste = sterile; Pvl = protruding vulva; Muv = multivulva; Vab = variable abnormal; Clr = clear, translucent appearance; Sma = small body size; Dpy = dumpy body shape; WT = wild-type (normal) appearance. (D) Number of gut nuclei varies in late L4 stage animals. The images show sample fluorescence of a *pept-1*::mCherry::H2B reporter in each of the two strains. The bar chart shows that surviving *end-1,3(MED-)* L4-stage animals have a variable number of gut nuclei and a higher mean overall. 24 control and 50 *end-1,3(MED-)* animals were scored. Anterior is to the left in panels (A) and (D), which are also at the same scale. The normal adults are approximately 1mm long.

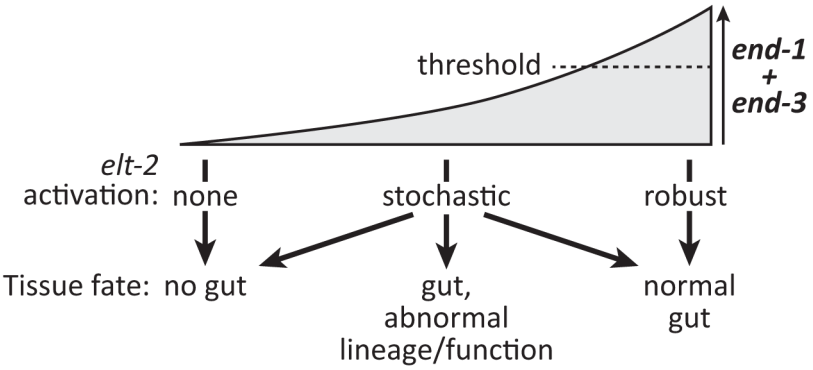

Fig. 7.

Speculative model of how the combined activities of *end-1* and *end-3* must reach a threshold for completely normal E lineage development. Below that threshold, specification may still occur, but it becomes stochastic, in some cases allowing only a subset of E descendants to adopt an intestine fate. Those that have made a relatively normal gut may manifest defects in intestine function at the adult stage. In the complete absence of *end-1* and *end-3* together, gut specification fails (Owraghi et al., 2010).

Table 1

Endoderm production in *C. elegans* strains

Genotype	% of Embryos with Gut (n)*
Wild-type (N2)	100% (n>500)**
end-1(ok558)	100% (322)**
end-3(ok1448)	95% (155)**
end-1(ok558) end-3(ok1448)	0% (190)**
*end-1,3(−)****; *Si[end-1(+)]*	96% (133)
end-1,3(−); Si[end-1(MED-)]	28% (98)
end-1,3(−); Si[end-3(+)]	100% (87)
end-1,3(−); Si[end-3(1+2+3+4-)]	100% (253)
end-1,3(−); Si[end-3(1-2-3-4+)]	85% (271)
end-1,3(−); Si[end-3(MED-)]	0% (93)
end-1,3(−); Si[end-1(+)]; Si[end-3(+)]	100% (169)
end-1,3(−); Si[end-1(MED-)]; Si[end-3(+)]	100% (139)
end-1,3(−); Si[end-1(+)]; Si[end-3(MED-)]	100% (214)
end-1,3(−); Si[end-1(MED-)];Si[end-3(MED-)]	75% (459)
itDf2	0% (123)
itDf2; Si[end-1(+)]; Si[end-3(+)]	100% (126)
itDf2; Si[end-1(MED-)]; Si[end-3(MED-)]	75% (198)

* scored by presence of any amount of gut granules visualized by polarized light birefringence.

** from Owraghi et al., 2010, included here for comparison.

*** *end-1,3(−)* denotes the *end-1(ok558) end-3(ok1448)* double-mutant genotype.

Table 2

Endoderm specification in *skn-1*, *pop-1* and *pal-1* RNAi-treated transgenic strains

Genotype and RNAi treatment	% of Embryos with Gut (n)*
end-1,3(−); Si[end-1(+)]; Si[end-3(+)]	100% (169)
end-1,3(−); Si[end-1(MED-)];Si[end-3(MED-)]	75% (459)
end-1,3(−); Si[end-1(+)]; Si[end-3(+)]; skn-1(RNAi)	30% (454)
end-1,3(−); Si[end-1(MED-)]; Si[end-3(MED-)]; skn-1(RNAi)	21% (522)
*end-1,3(−); Si[end-1(MED-)]; Si[end-3(MED-)]; skn-1(RNAi)***	27% (218)
end-1,3(−); Si[end-1(+)]; skn-1(RNAi)	4% (416)
end-1,3(−); Si[end-3(+)]; skn-1(RNAi)	3% (259)
end-1,3(−); Si[end-1(+)]; Si[end-3(+)]; pop-1(RNAi)	100% (564)
end-1,3(−); Si[end-3(+)]; pop-1(RNAi)	100% (272)
end-1,3(−); Si[end-1(MED-)]; Si[end-3(+)]; pop-1(RNAi)	99% (225)
end-1,3(−); Si[end-3(1+2+3+4-)]; pop-1(RNAi)	100% (222)
end-1,3(−); Si[end-1(+)]; Si[end-3(MED-)]; pop-1(RNAi)	6% (489)
end-1,3(−); Si[end-3(1-2-3-4+)]; pop-1(RNAi)	1% (345)
end-1,3(−); Si[end-1(+)]; pop-1(RNAi)	0% (74)
end-1,3(−); Si[end-1(MED-)]; Si[end-3(MED-)]; pop-1(RNAi)	0% (319)
*end-1,3(−); Si[end-1(MED-)]; Si[end-3(MED-)]; pop-1(RNAi)***	5% (352)
end-1,3(−); Si[end-1(+)]; Si[end-3(+)]; pal-1(RNAi)	100% (400)
end-1,3(−); Si[end-3(+)]; pal-1(RNAi)	100% (370)
end-1,3(−); Si[end-1(MED-)]; Si[end-3(+)]; pal-1(RNAi)	100% (671)
end-1,3(−); Si[end-1(+)]; Si[end-3(MED-)]; pal-1(RNAi)	80% (610)
end-1,3(−); Si[end-1(+)]; pal-1(RNAi)	58% (404)
end-1,3(−); Si[end-3(1-2-3-4+)]; pal-1(RNAi)	55% (276)
end-1,3(−); Si[end-1(MED-)]; Si[end-3(MED-)]; pal-1(RNAi)	3% (755)
*end-1,3(−); Si[end-1(MED-)]; Si[end-3(MED-)]; pal-1(RNAi)***	1% (372)

* scored as in Table 1.

** Gonadal injection of dsRNA performed as described (Maduro et al., 2005b). All other knockdowns were by bacterial feeding-based RNAi (Kamath et al., 2001).